Self-Shadowing Effects on the Thermal-Structural Response of Orbiting Trusses

Jack Mahaney*
Mercer University, Macon, Georgia
and
Earl A. Thornton†
Old Dominion University, Norfolk, Virginia

An investigation of self-shadowing effects on the thermal-structural response of orbiting trusses is described. The shadowing, heating, thermal, and structural analyses are summarized. The significance of shadowing on the thermal-structural behavior of a single member and a section from the center column of the Gravity Gradient Space Station is described. For the trusses considered, the study shows that member self-shadowing effects significantly alter the behavior and must be included to predict the thermal-structural response with high precision.

Nomenclature

A	= truss member cross-sectional area
A_i	= member surface area for incident radiation
A_r	= member surface area for emitted radiation
c	= specific heat
d	= member diameter
D	= distance between shadower and shadowed member
E	= modulus of elasticity
F_T	= equivalent member thermal force, Eq. (4)
i	= typical submember
k	= thermal conductivity
L	= member length
$\dot{q}$	= heating rate
S	= solar vector
SHAD	= solar heating attenuation factor
t	= time
T	= temperature
T_{avg}	= average member temperature
V	= member volume
x,y,z	= local Cartesian coordinates
X,Y,Z	= global Cartesian coordinates
α	= thermal expansion coefficient
ϵ	= surface emissivity
ρ	= density
σ	= Stefan-Boltzmann constant
θ	= orbital position
$\Delta\theta$	= shadowing duration

Subscripts

a	= Earth albedo
e	= Earth
H	= horizontal shadow
NH	= nonhorizontal shadow
ref	= reference (i.e., T_{ref})
s	= solar

Presented as Paper 84-1765 at the AIAA 19th Thermophysics Conference, Snowmass, CO, June 25-28, 1984; received Aug. 1,1985; revision received Sept. 23, 1986.

*Assistant Professor, Mechanical and Aerospace Engineering Department. Member AIAA.

†Professor, Mechanical Engineering and Mechanics Department. Senior Member AIAA.

Introduction

LARGE space structures present engineers with significant challenges in analysis and design. The large size of the structures distinguishes them from past Earth satellites. Deployable antenna concepts up to 100 m in diameter and even larger erectable structures are under consideration. For lower weight and high stiffness, design concepts often employ space trusses. To minimize weight and thermal distortions, the designs extensively use advanced composite materials. Even with advanced composites, an important design constraint is to control structural deformations within close tolerances. For example, the surface of an antenna must typically be maintained to within 1% of the wavelength to maintain adequate pointing accuracy and signal quality. Such stringent operational requirements have focused attention on analysts' capabilities of predicting small deformations with high accuracy.

The control of deformations of large space structures within small tolerances requires careful consideration of several effects on the structural response. Reference 1 assesses recent advances in the thermal-structural analysis of large space structures. Important areas for thermal-structural research are identified, including spacecraft self-shadowing effects on the structural response. The consideration of shadowing by slender, opaque structural members has been customarily omitted for latticework structures such as trusses. This assumption has been questioned,[2] particularly for nearly planar, Earth-facing structures. For these structures, significant shadowing can occur when the solar vector is nearly tangent to the orbit. The prediction of slender-member shadowing effects is quite complex and may be expensive for a truss with hundreds of members. Consequently, an understanding of the effect of slender-member shadowing on the thermal-structural response is needed to determine the extent to which shadowing should be included in the design process.

The purpose of this paper is to describe a recent investigation of slender-member self-shadowing effects on the thermal-structural response of orbiting trusses. The heating, thermal, and structural analysis of orbiting trusses considering shadows will be described first. Types of shadows and the determination of shadow occurrence will be discussed. Methods for computing the attenuated heat loads and member thermal-structural response will be described. The significance of shadowing on the thermal-structural behavior of a single truss member and a complete truss will then be presented.

Analysis

Heating

An orbiting truss may be heated by environmental and onboard heat sources. The sun and the Earth are the primary environmental heat sources. Onboard heating may come from many sources such as prime power systems, electronic packages, and heat rejection systems. To study self-shadowing effects, only environmental sources will be considered herein. The environmental heating of a structure in Earth orbit changes with time; the heating is a function of the orbit altitude and the structural member orientation with respect to the sun and Earth. The heating rate $\dot{q}$ is the sum of the solar heating rate $\dot{q}_s$, the Earth-emitted heating rate $\dot{q}_e$, and the Earth albedo heating rate $\dot{q}_a$. Member-to-member shadowing attenuates the solar heating rate on the shadowed member. Shadowing from Earth and albedo heating can be neglected because of the relatively large size of the Earth compared to typical member dimensions.[3] The attenuation of solar heating is represented herein by an attenuation factor, SHAD. Thus, when shadowing is considered, the member heating rate is

$$\dot{q} = \text{SHAD} * \dot{q}_s + \dot{q}_e + \dot{q}_a \qquad (1)$$

If no shadowing occurs, SHAD = 1; for complete umbral shadowing, SHAD = 0. The methods used for computing $\dot{q}_s$, $\dot{q}_e$, and $\dot{q}_a$ appear in Ref. 5.

Slender-Member Shadowing

For convenience, member-to-member shadows are classified as either cross- or parrallel-member shadows. The classification of cross- and parallel-member shadows is a useful distinction for understanding shadowing effects on truss thermal-structural response, but the classifications are not used for the actual computation of the attenuation factor, which is based on a submember approach. A shadowed member may experience one or more cross-member shadows. Cross-member shadow widths are small compared to member lengths and the effects are quite transitory because the shadows move along the shadowed member as the truss changes orientation. Parallel-member shadows progress over a member until the entire member is shadowed. The duration of a cross-member shadowing event is typically much larger than the duration of a parallel-member shadowing event. The occurrence of shadowing depends strongly on the truss geometry, member dimensions, and truss orientation with respect to the solar vector.

The determination of the occurrence of a shadowing event, the type of shadow, and the attenuation factor SHAD is made using a modified version of the procedure described in Ref. 2. To simplify the analysis in this study, the truss orbit is assumed to be in the ecliptic plane defined by the Earth's orbit about the sun. Figure 1 shows the orientation of a small truss with respect to a global XYZ system and the solar vector S. In the orientation shown in Fig. 1a, member IJ may experience cross-member shadows from two shadowers, A and B. In Fig. 1b, member IJ may experience parallel-member shadows from three shadowers. To determine the detailed development of the shadows on a member IJ, the member is subdivided into a number of submembers and the shadowing history of each submember is analyzed. The analysis is performed using a local xyz system located at the center of gravity of submember i. For convenience, the local x-z plane is oriented parallel to the global X-Z system. Figure 2 shows the orientation of a typical submember i in the local xyz system and two potential shadowers, A and B.

Because of the local coordinate system definition, any shadower must either pierce or lie in the x-z plane. The product of the y coordinates of joints 1 and 2 of a shadower will therefore be less than or equal to zero. Two kinds of shadowers must be considered: nonhorizontal shadowers and horizontal shadowers. If $y_1 * y_2$ is less than or equal to zero, the

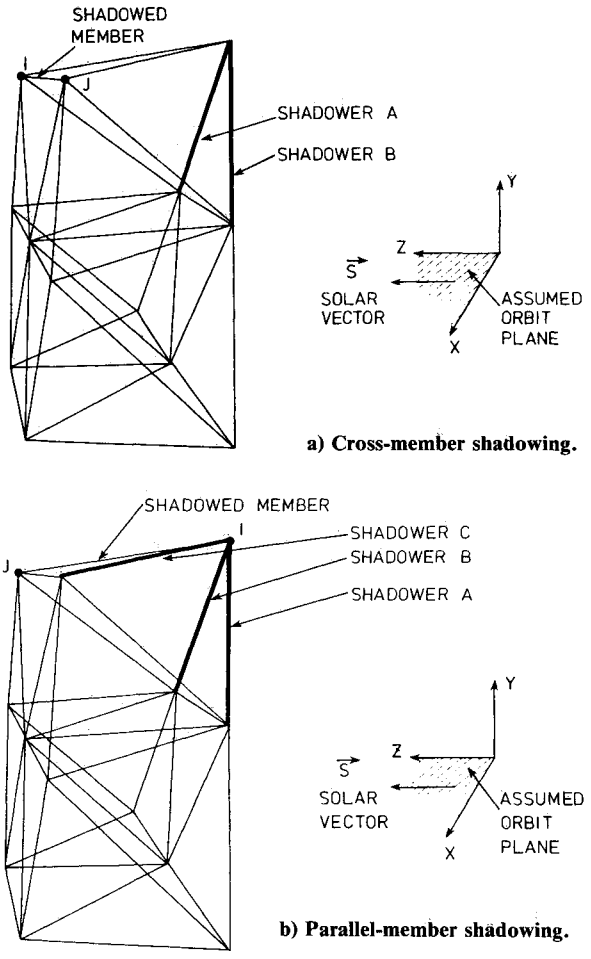

Fig. 1 Truss member shadowers and shadowed members.

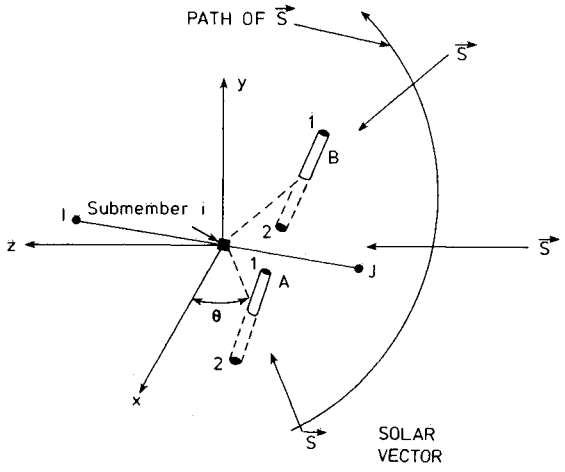

Fig. 2 Orbital positions of shadowers of submember 1.

shadower pierces the x-z plane and is nonhorizontal. If $y_1 = y_2 = 0$, the member lies in the x-z plane and the shadower is horizontal. Once the shadowers are identified as horizontal or nonhorizontal, the orbital positions at which they shadow submember i can be determined.

The orbital position θ (see Fig. 2) at which a nonhorizontal member shadows submember i is computed from the coordinates of the point where the shadower pierces the x-z plane. The duration of shadowing $\Delta\theta_{NH}$ depends on the shadower diameter, the distance between the shadowed member and the shadower, the angle that the shadower makes with respect to the x-z plane, and the angle subtended by the solar disk.

Since a horizontal shadower lies in the x-z plane, the shadowing duration $\Delta\theta_H$ will be much greater than for a nonhorizontal shadower. The duration of shadowing $\Delta\theta_H$ depends on the shadower length, the distance between the shadowed member and the shadower, the orientation of the shadower in the x-z plane, and the angle subtended by the solar disk.

Shadow occurrence and duration are now known for each submember and identify the intervals in the solar heating rate history during which the heating rate is to be reduced by the attenuation factor SHAD. SHAD is the percentage of solar radiation that reaches submember i and is used to account for umbral and penumbral shadowing effects. For umbral shadowing, SHAD = 1.0 and no solar radiation reaches the shadowed subelement. When penumbral shadowing occurs, SHAD is less than 1.0. SHAD is determined by calculating the percentage area of the solar disk that is covered by the projection of the shadower. SHAD depends on the distance D between the shadowed member and shadower, the shadower diameter d, the radius of the sun, and distance to the sun. For a nonhorizontal member, SHAD varies as a member moves across the solar disk. The variation of SHAD during a nonhorizontal-member shadowing event is shown in Fig. 3 for various D/d ratios. The figure shows that for small D/d values SHAD is zero (complete attenuation) over most of the shadowing event, but for large D/d values SHAD varies throughout the event. To simplify the computations for a nonhorizontal shadowing event, an average SHAD is calculated by applying numerical integration to the appropriate D/d curve and the average SHAD is used over the duration of the event. For a horizontal member, SHAD is very nearly constant during the shadowing event, and it is assumed constant herein.

Thermal

The heat-transfer problem for an orbiting truss includes nonlinear radiation exchanges, temperature-dependent thermal properties, and temperature gradients along member lengths and over member cross sections. In this study, thermal properties are assumed constant, member-to-member radiation exchanges are neglected, and temperatures are assumed uniform over member cross sections. These assumptions are reasonable for detrmining the overall thermal-structural response,[3] including shadowing effects. A recent thermoelastic study[4] of composite space trusses includes circumferential conduction and internal radiation effects. These effects introduce thermal bending moments, but for the truss members considered, the study showed that axial forces were the predominant thermal loading. The thermal problem is nonlinear due to emitted radiation and is transient due to the time-varying heating.

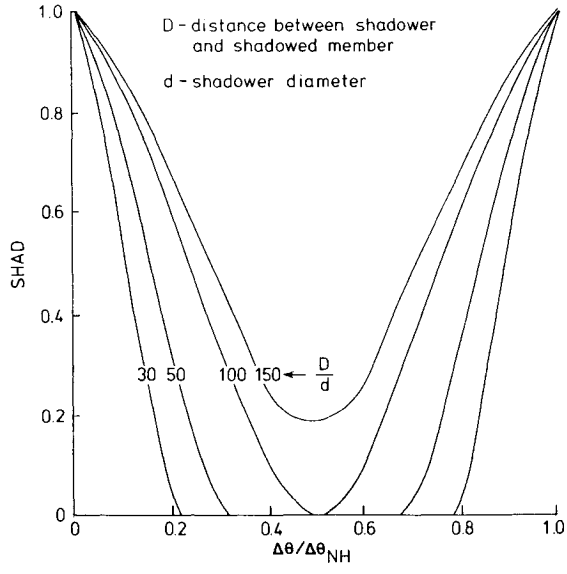

Fig. 3 Variation of nonhorizontal SHAD during shadowing event for various D/d ratios.

For a composite truss member subject to uniform heating (i.e., no shadowing), the temperature is nearly constant and axial conduction heat transfer is neglible.[5] Thus, neglecting shadowing, each truss member can be modeled as a single isothermal member. An isothermal member has only one temperature unknown $T(t)$ and the equations are uncoupled and can be solved independently. The isothermal member temperature is computed by solving the conservation of energy equation

$$\rho cV\frac{\partial T}{\partial t}+\epsilon\sigma A_r T^4 = A_i\dot{q} \tag{2}$$

where ρ is the material density, c the specific heat, V the member volume, ϵ the surface emissivity, σ the Stefan-Boltzmann constant, A_r the radiation surface area, and A_i the incident radiation area.

When a composite truss member is shadowed, it is no longer isothermal since the temperature is lower in the shadows and conduction occurs along the member. The details of the shadowed members' axial temperature distribution must be determined to predict the structural response accurately. The member temperature $T(x,t)$ is computed by solving the conservation of energy equation

$$\rho cV\frac{\partial T}{\partial t}-kA\frac{\partial^2 T}{\partial x^2}+\epsilon\sigma A_r T^4 = A_i\dot{q} \tag{3}$$

where k is the thermal conductivity and A the cross-sectional area. Equation (3) is solved using the finite-element method[6] with one element per submember used in the heating analysis. To determine the detailed spatial temperature variation, several unknown nodal temperatures per member must be computed.

Structural

Since the temperature is assumed uniform over a member cross section, only axial forces are developed. Each truss member can be represented by a single structural rod element. Structural inertia effects are neglected so that a quasi-static structural analysis can be performed at selected times in the thermal response.

The effects of the member temperature distribution are included in the structural analysis through the equivalent member thermal forces $F_T(t)$. The member equivalent thermal forces are computed from

$$F_T(t) = AE\alpha[T_{\text{avg}}(t) - T_{\text{ref}}] \tag{4}$$

where E is the modulus of elasticity, α the coefficient of thermal expansion, $T_{\text{avg}}(t)$ the average member temperature, and T_{ref} the reference temperature for zero stresses. The average member temperature is

$$T_{\text{avg}}(t) = \frac{1}{L}\int_0^L T(x,t)\,dx \tag{5}$$

where the integration is over the length L of a member. If a member is not shadowed, the average member temperature is the isothermal member temperature and no integration is needed. If a member is shadowed, then the integral is evaluated by integration over all submembers.

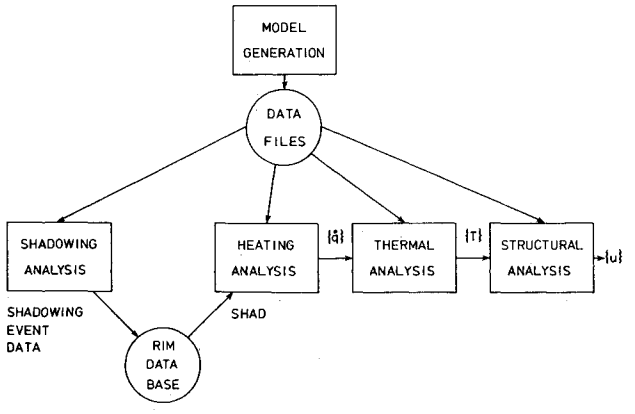

Fig. 4 Summary of computational procedure.

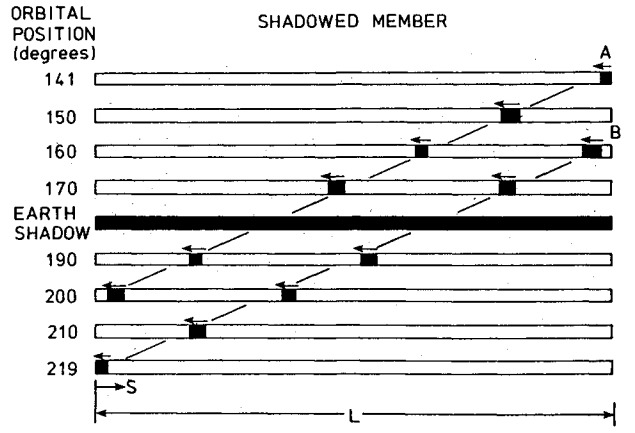

Fig. 5 Cross-member shadow movements.

Computational Procedure

The computations are performed using five programs to generate models and perform the shadowing, heating, thermal, and structural analyses. Figure 4 summarizes the computational procedure. The heating, thermal, and structural analyses use the finite-element method based on a common geometric model. The relational data manager[7] RIM is used to retrieve the attenuation factors SHAD from the shadowing event data generated by the shadowing analysis.

Self-Shadowing Effects

To determine self-shadowing effects on the thermal-structural responses of orbiting trusses, three examples are analyzed. The first two examples treat single members and provide insight into member behavior due to cross- and parallel-member shadows. The last example considers a section from the center column of the Gravity Gradient Space Station, and provides insight into the response of a complete structure. The truss members in the first two examples are graphite-epoxy tubes with lengths of 6 m and diameters of 0.1 m. The truss members are in a geosynchronous, Earth-facing orbit in the ecliptic plane.

Cross-Shadowed Member

Figure 1a shows a truss with member IJ that experiences cross-member shadowing from two shadowers A and B. A shadowing analysis using 100 submembers shows that the shadowing of the member begins at the orbital position $\theta = 141$ deg and continues through $\theta = 219$ deg. Figure 5 shows the movement of the two shadows across the member. Note that, during the cross-member shadowing event, the member also passes through the Earth shadow and becomes completely shadowed. The temperature response of the point $S/L = 0.9$ on the member is shown in Fig. 6. The two sharp dips in the member temperature history just before entering the Earth shadow indicate the passage of the shadows across the point. Figure 7 shows the member temperature distribution at $\theta = 170$ deg. The lower temperatures in the two shadowed regions indicate the thermal effects of the shadows. The regions of lower temperatures are wider than the shadowed regions because of conduction and transient effects.

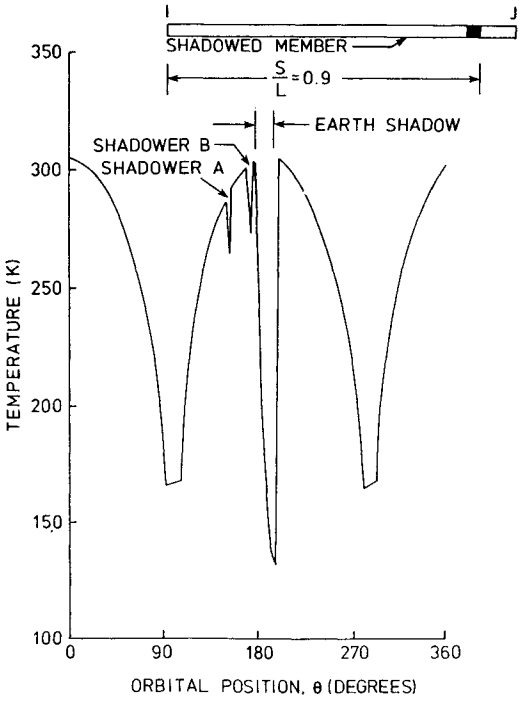

Fig. 6 Temperature response of cross-shadowed members at $S/L = 0.9$.

The member deformation distribution at $\theta = 170$ deg is shown in Fig. 8. The temperatures at this orbital position are lower than those at the satellite noon position when the member is directly between the sun and Earth. The noon reference temperature is 304.8 K and the member contracts. Without cross-member shadowing, the member has a very small contraction (0.015 mm) because the member temperature (302.8 K) is very close to the reference temperature. The shadowed regions have pronounced local effects on the deformation and increase the contraction by 0.023 mm. The effects of the shadows in this case are quite large as a percentage, since the unshadowed member contraction is small.

Parallel-Shadowed Member

Figure 1b shows a truss with member IJ that experiences parallel-member shadowing from shadowers A, B, and C. A shadowing analysis with 100 submembers shows three distinct occurrences of member-to-member shadowing: 1) shadowing by B at $\theta = 190$–210 deg, 2) shadowing by A at $\theta = 210$–230 deg, and 3) shadowing by C at $\theta = 250$–290 deg. Figure 9 shows the development of the shadows on the member IJ due to shadower B. The shadow advances from end $S = 0$ until the member is completely shadowed at $\theta = 202$–203 deg and then the shadow regresses until it nearly completely disappears at 210 deg. For a very short section near $S = 0$, the shadow duration is actually longer, but since joints are neglected in the analysis end effects are ignored. The figure shows the shadow growth to occur in increments rather than continuously because of the orbital increments used in the analysis. Figure 10 shows the member temperature distribution at $\theta = 203$ deg when the member is completely shadowed. The drop in temperatures follows the shadow movement across the

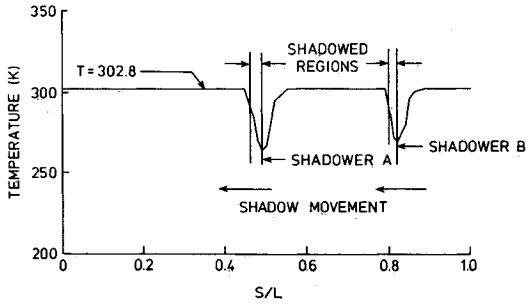

Fig. 7 Cross-shadowed member temperature distribution at orbital position 170 deg.

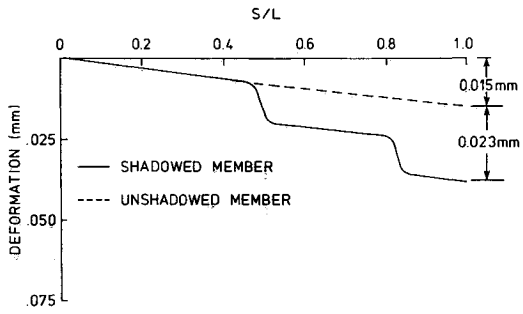

Fig. 8 Cross-shadowed member deformation distribution at orbital position 170 deg.

member. The steps in the distribution correspond to the incremental shadow movements. Lower temperatures occur near $S=0$ because this end is shadowed for the complete duration. The member deformation distribution at $\theta=203$ deg is shown in Fig. 11. The temperatures at this orbital position are lower than the noon reference position temperature of 265.7 K, and the member contracts. Without shadowing, the member has a contraction of 0.240 mm, which is increased significantly by the shadowing. Unlike cross-member shadowing, there are no pronounced local shadowing effects because the shadowing occurs over the entire member. The effects of the shadows more than double the total member contraction.

Gravity Gradient Space Station

The final analysis was performed on a part of the Gravity Gradient Space Station (Fig. 12), a concept being studied by NASA. The station contains a central column to which are attached power panels and radiators near the top and various habitation and logistics modules near the bottom. The notation "Nadir" at the bottom indicates that the column continually points at the Earth. Since the station will be placed in a low orbit, the analysis described herein assumes an orbital altitude of 250 km in the ecliptic plane.

Figure 13 shows the portion of the central column below the modules. The total length of this portion is 42.67 m with a square cross section of 4.267 m on a side. This part of the truss was analyzed because it could be considered to be cantilevered from the much larger mass of the station above. In addition, during the part of the orbit analyzed there is only self-shadowing; the large structures above did not cast shadows on the lower section.

Since the truss orbits at a low altitude, the heating history is very different from that in a geosynchronous orbit. One reason is that the Earth-emitted and Earth-albedo heating can be a considerable fraction of the total heat load. In addition, the orbital period is much shorter (only 95 minutes), so that heat loads change faster than in the geosynchronous orbit. Finally, almost 37% of the orbit is spent in the shadow of the Earth. Thus, the only time the truss is in thermal radiation equilibrium is during the short period in the Earth's shadow

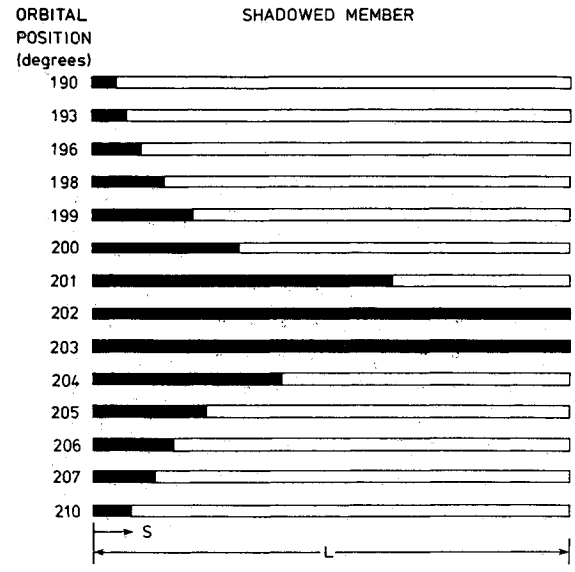

Fig. 9 Parallel-member shadow development by shadower B.

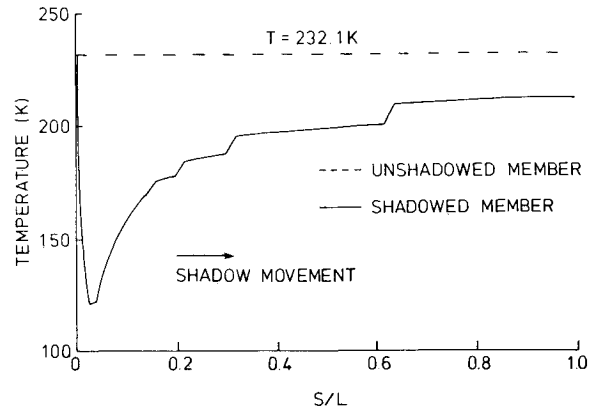

Fig. 10 Parallel-shadowed member temperature distribution at orbital position 203 deg.

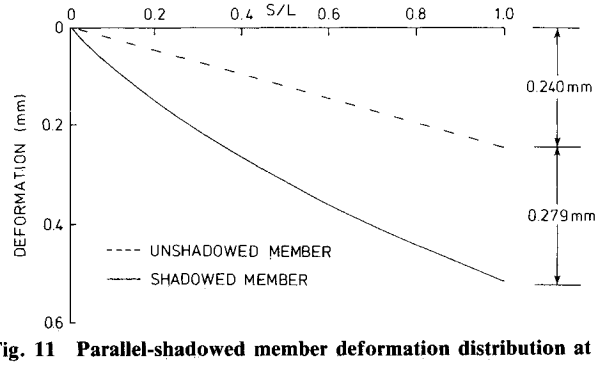

Fig. 11 Parallel-shadowed member deformation distribution at orbital position 203 deg.

just before entry into the sunlight. The analysis was thus begun in the shadow since the equilibrium condition provided convenient, reasonable initial conditions for the thermal analysis. The analysis described studied the behavior of the truss as it left the Earth's shadow and entered the sunlight. For the Gravity Gradient Space Station analyses, the shadowing, thermal, and structural analyses typically ran for less than 100 CPUs each on a CDC mainframe computer. The heating analysis took as much as 1000 CPUs, however, since it had to query and sort information form the RIM data base.

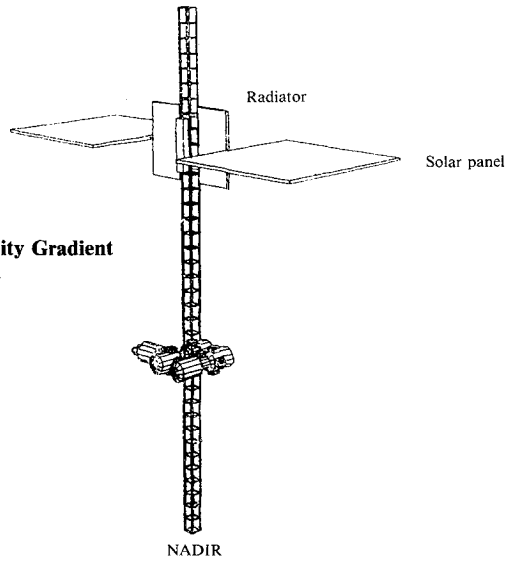

Fig. 12 Gravity Gradient Space Station.

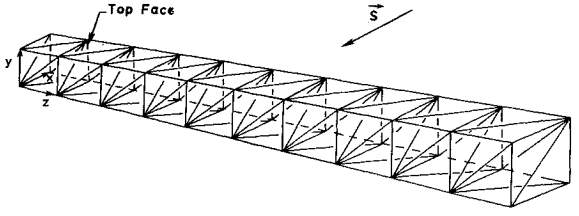

Fig. 13 Central column of Gravity Gradient Space Station.

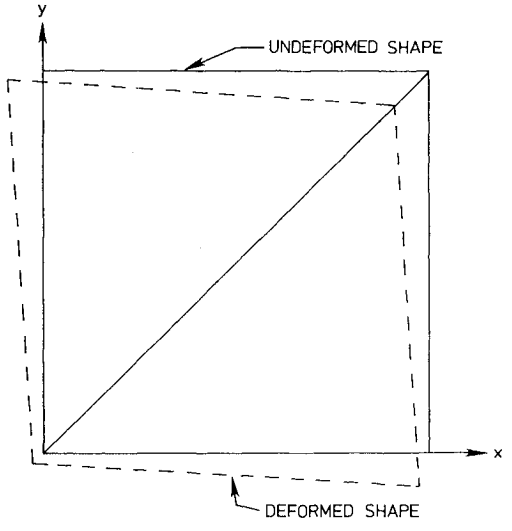

Fig. 14 Truss cross section at $\theta = 248$ deg.

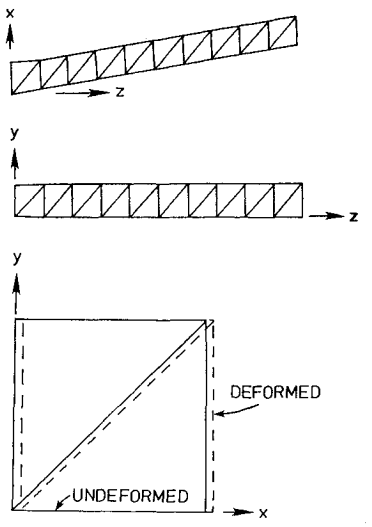

Fig. 15 Deformations of unshadowed truss at $\theta = 255$ deg.

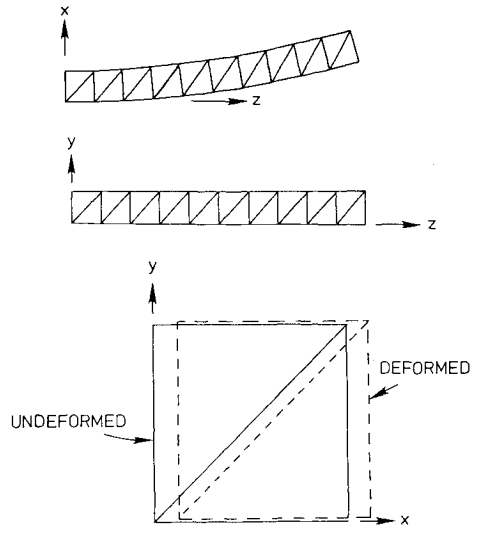

Fig. 16 Deformation of shadowed truss at $\theta = 255$ deg.

Figure 14 shows the cross section of the end of the truss in the shadow at orbital position $\theta = 248$ deg just before exit from the shadow. After being in the shadow, all member temperatures decreased to considerably less than the reference temperature of 294 K (70°F), being in the range of 212–190 K. Thus, all of the members contracted, the cross section deformed slightly as shown, and the total truss length decreased by 5.35 mm. The maximum x and y deformations at the tip were -0.57 mm and -0.15 mm.

Figure 15 shows the deformations of the truss at $\theta = 255$ deg, after Earth shadow exit, with shadowing neglected. The deformation of the top face is also shown. The bending occurs because the diagonal members receive less solar heating than the edge members. At this orbital position, then, their temperatures are still slightly below the reference temperature and they contract slightly, while the edge members are warmer than the reference temperature and they expand. The bottom face (not shown) behaves similarly. Figure 15 shows the face that is closer to the sun (up-sun) at $\theta = 255$ deg. Note the lack of in-plane deformations. Finally, Fig. 15 shows the cross section of the truss. The maximum deformations at the end of the truss are 2.37 mm in the x direction, 0.07 mm in the y direction, and 0.12 mm in the z direction.

Figure 16 shows the deformations of the truss at $\theta = 255$ deg when shadowing is considered. It also shows the bending of the top face. The bottom face (not shown) is similar. The bending is much more severe than in the unshadowed truss because the up-sun members shadow all of the other members in the face. Thus, the temperatures of the shadowed members remain the same as in the Earth's shadow, while the temperatures of the up-sun members increase. Thus, the up-sun members expand, while the down-sun members do not, and severe bending results. The tip of the truss has an x displacement of 23.2 mm. Since the rest of the members experience only a small amount of cross-member shadowing, the sun face and cross section experience little deformation. The tip deformations are 23.2 mm in the x direction, 1 mm in the y direction, and 1 mm in the z direction, showing that bending is the most important effect.

Conclusions

An investigation of self-shadowing effects on the thermal-structural response of orbiting trusses is described. The determination of a shadowing event is described and the method for computing the solar attenuation factor discussed. The heating, thermal, and structural analyses of an orbiting truss are summarized.

The significance of shadowing on the thermal-structural behavior of a single member is studied. The effects of two cross-member and parallel-member shadows on a single member are analyzed. The development of the shadow movements is documented, and the effects of the shadows on the member temperature distributions are shown. Cross-member shadows cause local drops in temperature along the shadowed member. These regions of lower temperature traverse the shadowed member for a portion of the orbit. The temperature drops are wider than the shadow widths because of conduction and transient heat transfer effects. Although the cross-member shadows make up only a small percentage of member lengths, the local decreases in temperature can cause member contractions that equal or exceed the contractions of the remainder of the unshadowed member. Parallel-member shadows cause a nonuniform drop in temperature along the entire member length. Parallel-member shadows begin to develop at either one or both ends of a member and the temperature drops at those points can be quite significant. The effect of parallel-member shadows on the structural deformation varies over its length. For the truss member studied, the member contraction was more than doubled by the parallel member shadowing.

Finally, a 42 m section of the central column of the Gravity Gradient Space Station was analyzed in a low-Earth orbit. In this case, the transition from the Earth's shadow to the sunlight caused bending to occur. The magnitude of the bending was increased tenfold (to 23 mm) when shadowing was considered.

For the trusses studied, the study shows that member self-shadowing effects significantly alter the thermal-structural response. The inclusion of shadowing complicates and increases the costs of the analyses, but the shadowing effect must be included to predict the thermal-structural response with high precision.

Acknowledgment

The authors are pleased to acknowledge that the research presented in this paper was supported by the Space Systems Division of the NASA Langley Research Center. We greatly appreciate the support and continued encouragement of the technical monitor, Dr. L. B. Garrett.

References

[1]Thornton, E. A. and Paul, D. B., "Thermal-Structural Analysis of Large Space Structures: An Assessment of Recent Advances," *Journal of Spacecraft and Rockets,* Vol. 22, July–Aug. 1985, pp. 385–393.

[2]O'Neill, R. F. and Zich, J. L., "Space Structure Heating: A Numerical Procedure for Analysis of Shadowed Space Heating of Sparse Structures," *AIAA Progress in Astronautics: Spacecraft Radiative Transfer and Temperature Control,* Vol. 83, edited by T. E. Horton, AIAA, New York, 1982, pp. 377–395.

[3]Chambers, B. C., Jensen, C. L., and Coyner, J. V., "An Accurate and Efficient Method for Thermal/Thermoelastic Performance Analysis of Large Space Structures," AIAA Paper 81-1178, June 1981.

[4]Lutz, J. D., Allen, D. H., and Haisler, W., "A Finite Element Model for the Thermoelastic Analysis of Large Composite Space Structures," AIAA Paper 86-0875, May 1986.

[5]Mahaney, J. and Strode, K. B., "Fundamental Studies of Thermal-Structural Effects on Orbiting Trusses," AIAA Paper 82-650, May 1982.

[6]Huebner, K. H. and Thornton, E. A., *The Finite Element Method for Engineers,* 2nd ed., Wiley, New York, 1982.

[7]Rogers, V. A., Sutter, T. R., Choi, S. H., and Blackburn, C. L., "Application of Data Management to Thermal/Structural Analysis of Space Trusses," AIAA Paper 83-1020, May 1983.